ELSEVIER

Surface Science 395 (1998) 168–181

surface science

Growth and morphology of Ni films on Cu(111)

Wulf Wulfhekel [a], Ingo Beckmann [a], Georg Rosenfeld [a,*], Bene Poelsema [b], George Comsa [a]

[a] *Institut für Grenzflächenforschung und Vakuumphysik, Forschungszentrum Jülich GmbH, D-52425 Jülich, Germany*

[b] *Faculty of Applied Physics and Centre of Materials Research, University of Twente, PO Box 217, 7500 AE Enschede, The Netherlands*

Received 9 May 1997; accepted for publication 30 July 1997

Abstract

Conventional and manipulated molecular beam epitaxy (MBE) of Ni on Cu(111) was studied by helium atom scattering and low-energy electron diffraction over a wide temperature range. During conventional MBE at low temperatures, three-dimensional rough growth is observed. The films consists of pyramids with {445} microfacets. At room temperature, growth leads to smoother films which consist of hexagonal structures. At high temperatures, the films partially grow via stepflow. To improve the film quality, growth manipulation methods, based on the concept of two mobilities, were applied. By temperature reduction or rate enhancement during nucleation and pulsed ion beam assisted deposition, the island number density was artificially increased and smoother growth of the first layers was promoted in most cases. However, temperature reduction during nucleation failed to promote better growth, which is explained by an unusual annealing behaviour of the nuclei. The morphology of films grown by manipulated and conventional MBE are compared. © 1998 Elsevier Science B.V.

Keywords: Atom–solid scattering and diffraction – elastic; Copper; Growth; Low energy electron diffraction (LEED); Nickel; Single crystal epitaxy

1. Introduction

One of the important aims of epitaxy is to produce smooth films on a substrate, but it is only in few cases that the deposited material grows in a layer-by-layer mode by nature. Even in many homoepitaxial systems, e.g. Ag/Ag(111) or Cu/Cu(111), multilayer growth (three-dimensional growth) is observed during molecular beam epitaxy (MBE) [1,2] due to growth conditions far from thermal equilibrium. In these systems, it is easy to increase the film quality by growth at higher temperatures, when the role of growth kinetics becomes less important and the increased mobility on the surface leads to a quicker equilibration to a thermodynamic stable configuration, i.e., a smooth surface. However, in heteroepitaxy, this growth recipe is often counterproductive. Here the system also equilibrates faster at higher temperatures, but due to different lattice constants and different surface energies of substrate and deposited material, the stable configuration in general consists of isolated crystallites [3], or even worse, the thermodynamically favoured state is an alloy of both materials. In homoepitaxy, the rough growth is due to the high probability that atoms landing on top of islands nucleate to form a higher layer before they can surmount the energy barrier at the islands edge [4,5] and fill the lower one.

* Corresponding author. Fax: (+31) 53 489.1101; e-mail: g.rosenfeld@tu.utwente.nl

PII S0039-6028(97)00622-5

Based on this kinetic picture, growth manipulation procedures are aimed at reducing the probability for nucleation on top of existing islands. This is done by using two different adatom mobilities, i.e., during nucleation a lower one than during subsequent growth [6]. In this way, an artificially high density of nuclei is formed during the early stage of monolayer growth while during subsequent growth the mobility remains high. Adatoms landing on top of these small islands prior to coalescence reach the edge of the island much more frequently in comparison to adatoms landing on the large islands formed during undisturbed nucleation. Hence, the probability that they surmount the step edge barrier and fill the lower layer before nucleating a second layer island is increased and layer-by-layer growth can be obtained [7,6,8].

These procedures, already successfully applied to the homoepitaxial systems Ag/Ag(111) [7], Cu/Cu(111) [9] and Pt/Pt(111) [10,11], should also lead to better heteroepitaxial films at low or intermediate temperatures, where the multilayer growth of the film is mainly determined by kinetics and a transition to the undesired and rough thermodynamically favoured state is hindered. In the manipulation experiments in this paper, we tried to apply these recipes to the heteroepitaxial system Ni/Cu(111).

Due to the small misfit of only 2.5%, Ni grows in pseudomorph layers up to film thicknesses of 7 ML on Cu(111) and then relaxes via the formation of dislocations [12–14]. No stacking faults at the interface could be observed by means of X-ray photoelectron diffraction and LEED [14,15]. However, growth does not proceed in a layer-by-layer manner and the films roughen quickly with thickness [16]. Electron energy loss spectroscopy experiments show that during the early stages of growth, intermixing of Ni and Cu starts at the interface at temperatures as low as 375 K while at even higher temperatures, the Ni film is covered with a cap-layer of Cu [17]. The aim of the growth manipulation experiments in this paper is to clarify whether growth can be improved using the concept of two mobilities at temperatures well below this intermixing and hence produce flat films without massive intermixing.

This paper is divided into two major sections. Section 3 deals with the unmanipulated growth of Ni on Cu(111). The different growth modes are revealed using helium atom scattering (TEAS) and the morphology of the films is studied with spot profile analysis low-energy electron diffraction (SPALEED). In Section 4, the concept of two mobilities is used to manipulate the growth mode and the morphology of such prepared films is compared to the conventionally grown ones.

2. Experimental set-up

All experiments were carried out in an ultra-high-vacuum (UHV) chamber with a base pressure below 3×10^{-11} mbar. A 67 meV supersonic He beam was used for He scattering measurements of a transfer-width of $\approx$420 Å [9]. The scattering apparatus was also equipped with an Auger electron spectrometer (AES) and a SPALEED. A more detailed description of the set-up can be found elsewhere [18,19].

The sample is a high-quality Cu(111) single crystal with a miscut angle of $<0.1°$. It was cut by spark erosion then carefully polished and, in a first step, cleaned of sulphur and carbon by glowing in a hydrogen atmosphere at 1100 K. Then it was prepared in situ by repeated cycles of sputtering with 1.2 keV Ne^+ ions and annealing to 800 K until no contamination could be detected by means of AES, and TEAS measurements revealed a mean terrace width on the surface of over 1000 Å [9]. The sample temperature was measured using a Ni–CrNi thermocouple inserted into a cavity in the crystal. Nickel was evaporated from a disc onto the sample using a home-built electron bombardment evaporator. The high-purity Ni disc was cleaned by chemical etching followed by glowing in a hydrogen atmosphere at 1100 K and was thoroughly outgassed in UHV before the experiments. During deposition, the pressure stayed below 1×10^{-10} mbar. No contaminations in the deposited films could be found with AES. After each growth experiment, great care was taken to clean the substrate from all the deposited material by sputtering before annealing to prevent the aggregation of Ni in the substrate.

3. Conventional growth of Ni–Cu(111)

First we determined the scattering conditions for anti-phase and in-phase He scattering of Ni on Cu(111) from which the step height can be deduced. A small amount of nickel (0.3 ML) was deposited onto the surface at an intermediate temperature (250 K) at a rate of $R=0.02$ ML/s. The as-prepared nickel islands are mostly only one layer high. Then, by changing the angle of incidence ϑ, the scattering conditions were varied, i.e., a rocking curve was taken. Under anti-phase scattering conditions, the destructive interference of the substrate with the islands leads to a strongly reduced specularly reflected intensity. On the other hand, under in-phase conditions, the reflected He beam is insensitive to the island area leading to a maximal signal. Losses in the reflected intensity are only caused by diffuse scattering from defects like step edges or point defects. The inset of Fig. 1a displays the rocking curve. It clearly shows two maxima and one minimum corresponding to two in- and one anti-phase scattering conditions. From the scattering angles under the in- and anti-phase conditions, the height of the nickel–copper step as seen by TEAS is found to be 1.91 ± 0.03 Å.

3.1. Growth modes

To monitor the growth of the film, TEAS is used during deposition of the material, i.e., deposition curves are taken. For layer-by-layer growth (two-dimensional growth), oscillations of the He intensity appear under both diffraction conditions. Maxima in the intensity correspond to the completion of a layer, minima to deposition of an odd multiple of 0.5 ML, when the surface is roughest. For non-ideal layer-by-layer growth, the amplitude of the oscillations decay with film thickness. During multilayer growth, interlayer mass transport is insufficient and the surface becomes increasingly rough as the next layer starts to nucleate well before the lower layer is completed. This results in both in- and anti-phase He intensities decaying monotonically.

Figs. 1a and b display the deposition curves of unmanipulated growth at various temperatures. During deposition at a rate of $R=0.02$ ML/s, the normalized He intensity under anti-phase diffraction conditions ($S=2.5$) was recorded as a function of deposition time. At temperatures below 250 K (see Fig. 1a), the intensity falls monotonically during deposition, indicative of multilayer growth. At such low temperatures, interlayer mass transport is obviously inefficient. For growth temperatures between 250 and 350 K, a single oscillation is observed followed again by a monotonic decay. The first layer grows in an imperfect two-dimensional manner. However, subsequent layers grow in a multilayer mode as indicated by the slow decay. With rising temperature, the oscillation becomes more pronounced and the following decay becomes slower, indicating that growth is

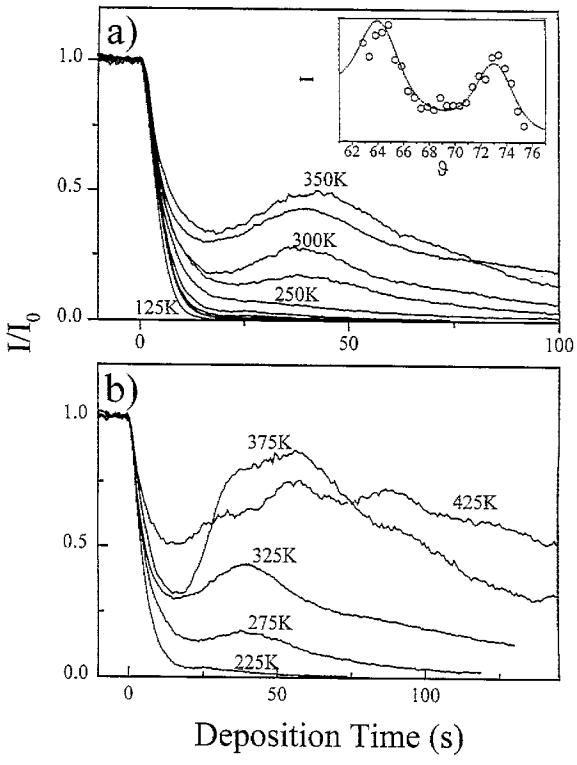

Fig. 1. Evolution of the normalized specular He intensity under anti-phase conditions ($S=2.5$) during deposition of Ni onto Cu(111) at a rate of $R=0.02$ ML/s. (a) Substrate temperatures varied between 125 and 350 K in 25 K steps; (b) substrate temperature varied between 225 and 425 K in 50 K steps. The inset displays the He intensity as a function of the scattering angle reflected from a surface onto which 0.3 ML of Ni has been deposited at 250 K. The maxima correspond to in-phase and minima to anti-phase scattering conditions.

smoother. Growth at these intermediate temperatures results in significantly smoother films compared with growth at low temperatures. Nevertheless, the films are still becoming rough, as can be seen by the low reflected intensity after more than 1 monolayer deposition. For temperatures above 375 K (see Fig. 1b), several decaying oscillations are observed. The amplitude of the oscillations, however, is small and the overall intensity remains rather high during growth. This behaviour may be explained by parts of the surface, i.e., the smaller terraces, growing in the step flow mode. On the larger terraces, nucleation, growth and coalescence of islands is taking place, resulting in the oscillations. However, detailed features like the amplitude of the first oscillation and the slight variation of the frequency of the oscillations are not explained by this. In particular, the fact that at 375 K a higher reflectivity than at 425 K and 1 ML coverage is observed, i.e. the film grown at a lower temperature is flatter, contradicts usual growth mechanisms. From other experiments, massive intermixing is known to start at these high temperatures [17] leading to complex intermixing kinetics, which most likely influences growth substantially. For a detailed study of the processes occurring at these high temperatures, a real space method is more appropriate. We therefore focus on the simpler growth situation below 375 K.

To gain insight into the initial processes of film growth, the island density as a function of temperature was measured. In the experiments, 0.3 ML Ni were deposited with a rate of 0.02 ML/s at a temperature between 135 and 260 K followed by cooling to ≈ 120 K to suppress further diffusion. Anti-phase peak profiles, taken at that temperature, displayed a broadening due to the islands on the surface. According to the method described in [20,21], the resulting average island densities were estimated from a fit to the broadened peak profiles. Fig. 2 displays an Arrhenius plot of the island number density. With rising temperature, a decrease in the island number density is observed, as expected from the classical nucleation theory [22,23]. The island density n is given by $n \propto \exp(iE_d + E_i)/((i+2)kT)$, where i is the size of the critical nucleus, E_d is the adatom diffusion energy on the terrace, E_i is the binding energy of

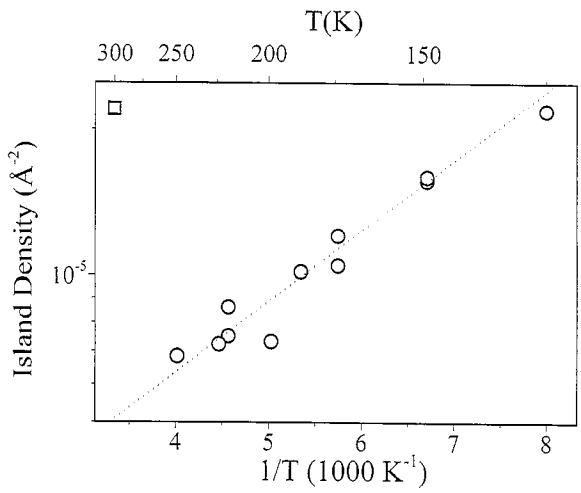

Fig. 2. Arrhenius plot of the mean island density at 0.3 ML coverage as a function of temperature for Ni islands grown on Cu(111). Deposition was carried out at a rate of $R = 0.02$ ML/s.

the critical nucleus, k is the Boltzmann factor and T is the temperature. Obviously the data can be well fitted with a straight line. There are no signs of a change in the size of the critical nucleus in the temperature range studied. Assuming that the dimer is stable ($i = 1$), the linear fit to the curve gives an adatom diffusion energy for Ni on Cu(111) of $E_d = 79 \pm 18$ meV. This is in reasonably good agreement with EMT calculations for this system of $E_d = 52$ meV [24] and also explains the roughly five times higher island densities observed in this system compared to results of similar experiments for the homoepitaxial systems of Cu(111) ($E_d = 30^{+10}_{-5}$ meV [9]) and Ag(111) ($E_d = 51 \pm 24$ meV [8]). There are reasonable arguments that the opposite assumption – that the Ni dimer is not stable in the temperature range studied – is unlikely to be true. First, EMT calculations [25] estimate the binding energies of Ni dimers and Pt dimers on their (111) surface to be of similar size and the Pt dimer is found to be stable up to ≈ 245 K [26]. The small misfit between Ni and Cu should not change the situation dramatically since an Ni dimer on the Cu surface most likely relaxes towards its bulk lattice spacing. Second, when $i = 2$ and a reasonable binding energy for the dimer are chosen (e.g. from EMT calculations [25]), the obtained diffusion energy is only

a fraction of the EMT value as well as the experimental values for similar homoepitaxial systems, which would imply faster diffusion and hence a much lower absolute island number density rather than the observed higher one.

3.2. Morphology

SPALEED, with its resolution and short data acquisition times, offers an elegant way to study the morphology of films in reciprocal space. Similar to TEAS, the scattering conditions (here the electron energy) for in- and anti-phase have to be found. It is not straightforward to extract the scattering phase from the intensity as a function of the electron energy. However, the width of the specular spot contains information about the scattering phase in a simple way. At in-phase scattering conditions, the spot is sharp, while at anti-phase scattering conditions, the specular peak is of maximal width. This also offers a simple method to determine the step height of the film. Provided that the energy-dependent phase shift between the deposit and the substrate is slowly varying compared to the phase shift caused by the interlayer distance, the step height can be determined [27].

Fig. 3 shows LEED peak profiles of the specular spot of surfaces onto which 1 ML of Ni were deposited at 140 K followed by a quench to 100 K. As already deduced from the TEAS measurements of the island density, the structures are small at these low temperatures and as a consequence, the effect on the variation of the peak width with energy should be large. All scans are 30% by 30% of the surface Brillouin zone (SBZ) in size. At certain electron energies, the observed peak is very sharp as in Figs. 3a and e, corresponding to in-phase scattering conditions. When raising the energy, the peak widens until three distinct facet reflexes become visible (see Fig. 3b) which move away from the specular peak and finally disappear and leave behind a very broad spot of low intensity (FWHM $\approx$ 10% SBZ) corresponding to anti-phase scattering condition (see Fig. 3c). When the energy is further increased, three facet reflexes show up again, but with a flipped orientation (Fig. 3d), move towards the central spot and eventually merge with it again at in-phase condition (Fig. 3e).

In Fig. 4, the scattering phase, S, of in-phase (squares) and anti-phase (circles) conditions, as determined by the sharpness of the spots, is plotted versus the square root of the electron energy. A

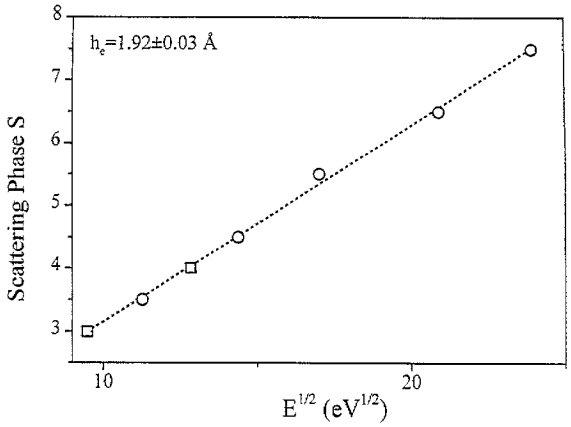

Fig. 4. Scattering phase S versus the square root of the incident electron energy determined from the broadening of peak profiles of 1 ML Ni deposited at 140 K. In-phase scattering conditions (□) have been determined from sharp specular peaks and anti-phase (○) from the flipping of the facet reflexes.

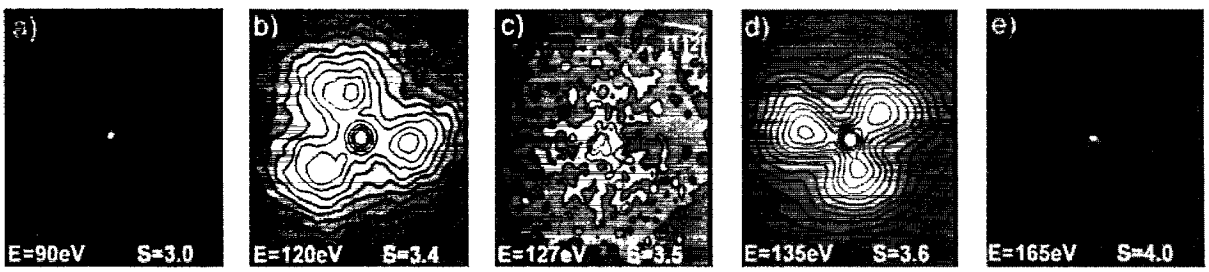

Fig. 3. LEED contour plots of the (00)-spot in linear intensity scale of 1 ML Ni deposited at 140 K with incident electron energies as indicated. The size of the scans are 30% by 30% of the surface Brillouin zone.

least-squares fit to the points yields the height of the Ni step on the Cu substrate to be 1.92 ± 0.03 Å, which coincides with the step height seen with TEAS.

From the fact that both diffraction techniques see the same step height, although LEED probes the core level electrons while TEAS only probes the outermost electrons due to a turning point ≈ 3 Å in front of the surface, it can be concluded that the interaction of He with the substrate and the film does not differ significantly as theoretical calculations predict [28] and that the differences in the energy-dependent phase shift between electrons scattered from a Ni and a Cu atom is negligible in the energy range studied.

Having determined the step height and the scattering phase, S, as a function of the electron energy, we return to the study of the morphology of the films deposited at low temperatures. From the fact that the observed diffraction pattern displays a three-fold symmetry with three facet peaks (Figs. 3b and d), one can directly deduce that the islands grown at such low temperatures show a three-fold symmetry, i.e. are of triangular shape or are build up of triangular parts and that a certain facet slope is selected during growth of the islands. However, the facet peaks are very broad (FWHM $\approx 10\%$ SBZ) indicating that the facets are irregular or of small extension or that a distribution of facets with slightly varying orientation is present. This finding agrees with the strong damping of the He intensity observed during growth, which is characteristic for a rough growth mode and small structures. The positions of the centre of the facet spots in k-space were surveyed as a function of electron wave number, i.e. a map of the facet rods in reciprocal space was made and is shown in Fig. 5. The measured positions (circles) are best fit with facets of a tilt angle of 6.0°, which is close to a {445} facet. Since the facet spots are rather wide, it is questionable to talk about well-ordered facets on the surface. However, there is a preferential slope of the multilayer islands of 6° and from the direction of the movement of the facet peaks with energy, one can conclude that mainly {100} step edges are present on the surface. The other possible closed-packed step edge, i.e. the {111} step edge, is not observed in the diffraction pattern. The same orientation of the facets have also been observed for films of 3 and 6 ML thickness within the uncertainty due to the rather diffuse peaks. In addition, for thicker films, the facet peaks become increasingly smeared out. It is unlikely, that at such low coverages as 1 ML, mechanisms like slope selection or kinetic roughening are already responsible for the specific slope observed. It seems to be more likely that the lack of interlayer mass transport in combination with a typical island separation is the reason for the slope. A good estimate for the typical slope of the sides of the triangular islands can be made by a simple geometric construction. Assuming a regular array of perfectly triangular islands with a separation taken from the estimation of the island density from the fit of Fig. 2, one obtains a facet angle of $\approx 4.2°$ which is in rather good agreement with the measurements. Certainly, the premise of perfectly triangular islands in a regular array is not fulfilled. A more rugged shape of the islands due to limited edge diffusion and scatter in the island size and separation caused by the statistical nature of nucleation may cause variations of the facet angle, which agrees with the large width of the facet reflexes. In addition, a minor systematic underestimation of the island density from the peak profiles may contribute to the slight deviation between simple geometric estimation and direct measurement of the typical slope.

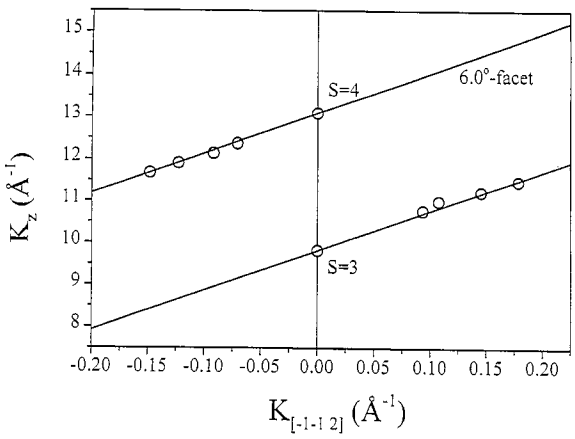

Fig. 5. Reciprocal space mapping of the facet reflexes of 1 ML Ni deposited at 140 K (○) and of a {445} facet (solid line).

The same orientation of the islands, i.e. the predominant existence of {100} step edges, has been found in the homoepitaxial growth of Pt(111) at a temperature range above fractal growth and below ≈450 K with STM [29] and of Cu(111) at low temperatures and low growth rates with SPALEED [30]. The finding of the same orientation of islands also in the heteroepitaxial case of Ni on Cu(111) suggests that a mechanism fundamental for fcc (111) surfaces is responsible for this. However, the predominance of {100} step edges does not reflect the equilibrium shape of the islands as shown in the case of Pt/Pt(111) by STM [29] and later in this paper for Ni/Cu(111) with SPALEED. The shape of the island is caused by temperature-dependent growth speeds of the two types of step edges. At low temperatures, the growth speed of the {111} step edges is faster than that of the {100} step edges so that in compact structures, the {111} step edges die out quickly and a triangular island or an island consisting of triangular parts with {100} step edges is formed.

When the growth temperature is raised, the situation changes. The specular LEED spot of 2 ML Ni deposited at 300 K displays a star-like diffraction pattern of six-fold symmetry in a wide energy range around anti-phase scattering conditions as can be seen in Fig. 6. At in-phase, a sharp spot-like diffraction pattern is observed, similar to those of Figs. 3a and e. Especially below (Fig. 6a) and above (Fig. 6c) the anti-phase condition, scattering in neither specific direction, corresponding to {100} and {111} type step edges, is dominating. Hence, both types of steps are equally present on the surface. No specific facet reflexes are found indicating that growth at that temperature does not lead to distinct facets. The FWHM at anti-phase scattering condition of 2.5% SBZ indicates that the film is far from being perfectly flat. The diffraction peak, consisting of a strong central spike and weak, broad wings of six-fold symmetry, may be explained by flat islands of either a superposition of both of the two possible orientations of triangular islands or more likely of a hexagonal shaped islands analogous to the islands observed on Pt(111) during homoepitaxy around 450 K [29], Cu(111) above 200 K [30] and Ag(111) at room temperature [31]. The phenomenon of a transition in growth shapes from {100} step edges at low temperatures to both types of steps edges at intermediate temperatures was also found in Pt(111) [29] and Cu(111) [30]. However, in the case of platinum, this transition is driven by the growth speeds of the two types of steps which are equal at intermediate temperatures where hexagonal islands are observed. When raising the temperature even higher, the growth speeds may even reverse and triangular islands with {111} step edges have been observed [29]. However, in the case of Ni/Cu(111), the change of the island shape is more likely to be driven by thermodynamical effects since annealing experiments show that already above 250 K, the three-fold symmetry of the specular spot transforms into a six-fold symmetry, as will be discussed later.

When choosing an elevated growth temperature above 375 K, considerable intermixing sets in, but as already deduced from the deposition curves of Fig. 1b, the reflectivity remains high during growth, i.e. the film grows two-dimensionally. In

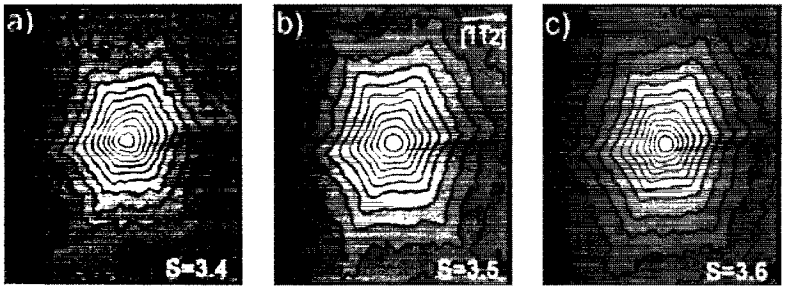

Fig. 6. LEED contour plot of the (00)-spot in logarithmic intensity scale of 2 ML Ni deposited at 300 K with scattering phase S as indicated. The size of the scans are 30% by 30% of the surface Brillouin zone.

accordance with this, the anti-phase spot of 2 ML Ni deposited at 440 K is with an FWHM of 1.3% SBZ rather sharp and featureless indicating a flat film (see Fig. 7a). This situation changes when the thickness is larger than 7 ML and dislocations build up to relax the film tension [13,14]. Fig. 7b shows the (00)-spot of ≈ 8 ML Ni deposited at 440 K. The peak has a three-fold symmetry and is with 13% SBZ extremely wide. Surprisingly, the width and shape does not depend on the scattering phase as expected from a rough layer. When varying S in the range of $S=3$–4, no major changes in the shape of the spot profile are detectable. This means that whatever is responsible for the widening of the peak, it is certainly not related to the elementary step height of the system or a height in the same order of magnitude. This widening is more likely caused by a mosaic structure or distortions due to the dislocations in the film.

4. Growth manipulation using the concept of two mobilities

To enhance interlayer mass transport and by this achieve layer-by-layer growth, the concept of two mobilities is used. By reducing the mobility of the adatoms during nucleation, an artificially high density of nuclei is created. Then growth is continued with a second and higher mobility so instead of few larger islands, many small islands grow on the surface. Adatoms landing on top of these small islands reach the edge of the island much more frequently, and hence the probability that they surmount the step edge barrier and fill the lower layer before nucleating a second layer island is increased.

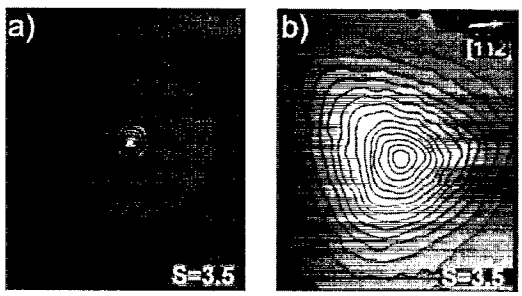

Fig. 7. Anti-phase ($S=3.5$) LEED profiles of the (00)-spot in a linear intensity scale of: (a) 2 ML; and (b) ≈ 8 ML Ni deposited at 440 K. The size of the scans are 30% by 30% of the surface Brillouin zone.

4.1. Growth manipulation via temperature alternation

A simple way to artificially increase the island number density is to perform the nucleation of islands at lower temperature than the rest of the monolayer growth. Since nucleation theory predicts an exponential decrease of the island density with temperature, this offers a very effective way to increase the island density. Such experiments in the homoepitaxial systems Ag/Ag(111) [7] and Cu/Cu(111) [9] lead to a significant improvement in interlayer mass transport resulting in layer-by-layer growth. Since also for Ni on Cu(111), the island density increases when deposition temperature is lowered, this recipe should lead to better growth. To test this procedure, firstly just enough material was brought onto the surface to accomplish the stage of nucleation, i.e. 0.1 ML, at low temperatures ranging from 70 to 220 K. Then the deposition was continued at higher temperatures between 200 and 300 K. Presuming that the nuclei survive the heating to the second temperature, the artificially raised island number density on the surface should result in an improved interlayer mass transport. However, none of the various deposition curves showed as strong oscillations as in the case of Ag/Ag(111) or Cu/Cu(111). No clear improvement in the growth could be obtained. On the contrary, as can be seen in Fig. 8, the normalized anti-phase He intensity reflected from the surface after the second stage of growth may even be lower than during natural growth, indicating that the film might even be rougher. Since lowering the temperature *does* also increase the island number density in the case of Ni on Cu(111), this discrepancy cannot be due to nucleation, but to an unusual annealing behaviour of the Ni islands created at low temperatures during heating to the growth temperature. To study this annealing behaviour, the specularly reflected in-phase intensity ($S=2$) of 0.3 ML Ni on Cu(111), deposited at 125 K, was recorded during

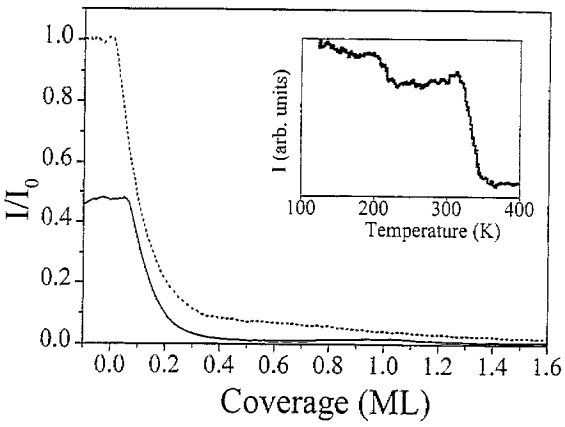

Fig. 8. Evolution of the normalized anti-phase He intensities during deposition of Ni at $T=245$ K onto Cu(111) surfaces, which were treated by pre-deposition of 0.1 ML Ni at 135 K (solid line) and for comparison during unmanipulated growth at T = 245 K (dotted line). Deposition was carried out at a rate of R = 0.02 ML/s. The inset displays the in-phase $S=2$ intensity during annealing of 0.3 ML Ni, deposited onto Cu(111) at 125 K, as a function of substrate temperature.

heating. The in-phase intensity is insensitive to the layer distribution and is only determined by the density of steps and point defects. Surprisingly, as can be seen in the inset of Fig. 8, the intensity drops in two steps slightly above 200 K and at $\approx$320 K, indicating that the surface roughens and either steps or point defects are created. This behaviour is the exact opposite of the one observed in the homoepitaxial systems Ag(111) and Cu(111) [7,9]. However, even in the case that the second temperature is chosen below the first annealing step, i.e. below 200 K, and the nucleation temperature as low as possible (70 K), only multilayer growth could be observed, which is most likely to be due to the rather low enhancement of island number density after this temperature variation and the low probability of adatoms to thermally surmount the step edge barrier at this low growth temperatures.

We also took SPALEED profiles in anti-phase scattering conditions during annealing. The information gained from these profiles is complementary to that from the in-phase TEAS annealing curve. The in-phase specular TEAS intensity is predominantly sensitive to step edges or point defects like adatoms or vacancies, while SPALEED profiles under anti-phase scattering conditions reflect the layer distribution. In contrast to the roughening of the film seen by TEAS, the SPALEED profiles of 1 ML Ni deposited at 115 K show the usual sharpening trend of the spots during annealing, as can be seen in Fig. 9. When heating up the sample, the spot initially narrows slightly, but still shows facet spots of three-fold symmetry (see Fig. 9b). This may be explained by a slight smoothing of the rather ragged islands reducing the scattering from the specular spot. When the temperature is further increased, the facet spots suddenly disappear at $\approx$265 K and leave a circular ring behind, as displayed in Fig. 9c. In addition, the three-fold symmetry disappears. Here, obviously, the predominance of the {100} step edges is lost and the islands begin to anneal to an equilibrium shape. The ring reflects the isotropic distribution of islands with a typical island separation set during nucleation. Further heating results in a rapid collapse of the ring diameter and the appearance of a background around the spot of clearly six-fold symmetry (see Figs. 9d and e). The islands now have six-fold symmetry and Ostwald ripening begins. The apparent discrepancy between the results of LEED and TEAS can easily be removed. It seems that during the annealing of the islands, point defects are created. In particular, at higher temperatures, the rearrangement of atoms on the surface can lead to intermixing and upward diffusion of Cu, driven by the lower surface free energy of Cu. These defects do not show up in the anti-phase LEED data, but may cause strong diffuse scattering in the in-phase TEAS measurements and may also act as nucleation centres in the second layer such that growth continued on annealed films results in multilayer growth instead of layer-by-layer growth. Therefore, in the case of Ni on Cu(111), the lower surface free energy of Cu leads to complications that prevent the successful application of temperature variation to obtain layer-by-layer growth. During heating to the second growth temperature, which typically takes several minutes, the surface is left to evolve towards thermal equilibrium by intermixing and the purely kinetic method of two mobility must fail.

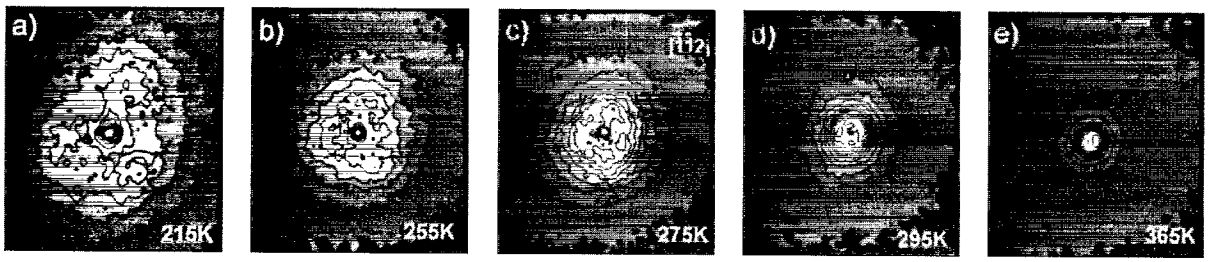

Fig. 9. Near anti-phase ($S=3.6$) LEED profiles of the (00)-spot in linear intensity scale, taken during annealing at temperatures as indicated, of 1 ML Ni deposited at 115 K. The size of the scans are 50% by 50% of the surface Brillouin zone.

However, from the fact that during annealing at temperatures around 275 K, the three-fold symmetry is already lost and a six-fold symmetry is achieved, one learns that these temperatures are sufficiently high to allow diffusion so that the triangular islands transform into hexagonal ones and the equilibrium shape of the islands is approached. Hence, also the six-fold symmetry of the (00) spot after growth at 300 K is most likely to be due to this equilibration of the island shape by diffusion along the step edges and not necessarily due to the growth speed of both types of steps being equal at that temperature. Obviously, the heteroepitaxial system of Ni/Cu(111) behaves different from the homoepitaxial case of Pt(111) where, at intermediate temperatures, hexagonal islands are also observed, but due to a different reason. In the case of Pt, a crossover of the growth speeds of the two step types occurs. Efficient diffusion for the equilibration of the island shape only sets in at substantially higher temperatures [29].

4.2. Growth manipulation via rate variation

A second way to increase the island number density during nucleation is to perform nucleation at a higher deposition rate than the subsequent growth. However, the island number density only slowly varies with the deposition rate $n \propto R^{i/(i+2)}$ as has been derived by Venables [22,23]. Hence, a rather large difference in deposition rates is required to achieve reasonably high enhancement factors for the island density. With our conventional electron bombardment evaporator, rate variations over two decades were possible, but did not lead to significantly better films. To achieve a very high flux during nucleation, a special evaporator was build consisting of thin high-purity Ni wires which were thoroughly outgassed in UHV. By discharging a large capacitor over one of the wires, it is instantaneously evaporated in an explosion resulting in a high deposition rate. The mass of the wires were chosen so that only less than 0.05 ML is deposited by the explosion. After nucleation of the islands in this way, the electron bombardment evaporator is used to continue growth. As can be seen in Fig. 10, which depicts the reflected anti-phase He intensity during such a growth experiment at 300 K, a stronger oscillation and a higher reflectivity at monolayer completion is achieved when rate modulation is used (solid

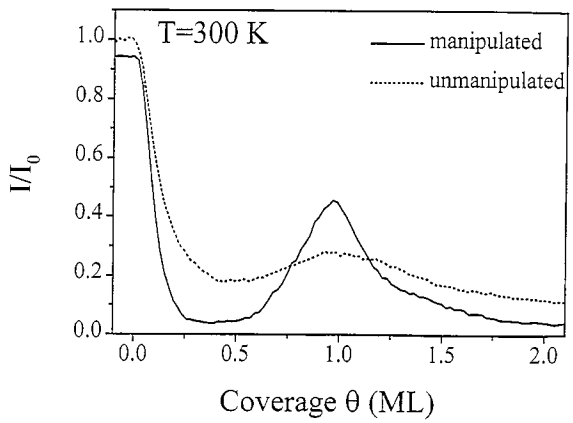

Fig. 10. Normalized anti-phase He intensity during deposition of Ni at 300 K onto a surface which was treated by predeposition at a high rate (solid line) and for comparison without predeposition (dotted line).

line) in comparison to the unmanipulated growth (dotted line), i.e. growth manipulation by a large rate variation does promote layer-by-layer growth and results in smoother films. Rate variation has the advantage that the surface is not left to evolve towards thermal equilibrium by intermixing since deposition with the second and lower rate can immediately be started after creating a high density of nuclei, in contrast to varying the substrate temperature.

This very cheap and simple method of exploding wires has the obvious disadvantage that for each manipulation you need a new wire. A more elegant way to modulate the deposition rate over many orders of magnitude offers the use of pulsed laser deposition for nucleation accompanied by conventional MBE for the growth of the rest of the monolayer. Here, the differences in rates may even be higher and hence even better layer-by-layer growth may be achieved.

4.3. Growth manipulation via ion beam pulses

A third way of creating an artificially high density of nuclei is to bombard the surface with ions prior to deposition or during the early stage of the growth of each monolayer. During sputtering, not only is material removed from the substrate leaving behind vacancies or vacancy islands in the topmost layer, but also adatoms are created on the topmost layer due to displacement of atoms by collisions or upward diffusion of interstitials created by collision cascades in the bulk. These often form one or several adatom islands close to the impact site, as has been observed in the case of Pt(111) by STM [8,11,32–34]. During growth on a slightly sputtered surface, these islands then serve as artificial nucleation centres during growth of the Ni films.

In a series of growth experiments at a substrate temperature of 300 K, freshly prepared surfaces were bombarded with a fluence between 0.8 and 8.2×10^{17} ions/m^2 of 1.2 keV Ne^+ ions corresponding to a sputtering of 0.015–0.16 ML [9]. Immediately after ion bombardment, Ni deposition was started at a rate of 0.02 ML/s. The normalized anti-phase He intensities recorded during manipulated and unmanipulated growth are shown for comparison in Fig. 11a. It can clearly be seen that ion bombardment with all the fluences used leads to a stronger oscillation and a higher reflectivity around 1 ML coverage compared with the unmanipulated case. This indicates a smoother growth of the film and a higher degree of filling of the first monolayer. Nevertheless, strong differences show up when varying the fluence. For the lowest fluence, the oscillation is enhanced only weakly. When the fluence is raised, the oscillation becomes stronger. For the highest fluence, however, the maximum intensity near layer completion is not the highest, but somewhat lower, which is most likely to be due to the surface structure after sputtering with such a high fluence. Since at the chosen substrate temperature sputtering does not lead to layer-by-layer but multilayer removal, a high fluence results in a surface structure with several open layers. In particular, the created vacancies or vacancy islands can no longer be neglected. These vacancies are only filled by direct deposition of atoms and not by downward diffusion of adatoms from the first layer since the material deposited on the first layer is immediately captured due to the high density of nuclei. This results in a lower reflectivity during growth. The best results are obtained for the intermediate fluence of 4×10^{17} ions/m^2 corresponding to a sputtering of 0.04 ML.

In addition, for fluences between 0.8 and 8.2×10^{17} ions/m^2, anti-phase peak profiles were taken after deposition of 0.5 ML of Ni at 300 K to estimate the island density. Within the error of measurement, they display the same island density as depicted by the square in Fig. 2. This island density was also observed for equivalent experiments in the homoepitaxial system of Cu/Cu(111) with fluences above 8×10^{16} ions/m^2 [9], where the island density created by sputtering saturates. It is not clear why in the case of Ni–Cu(111), a fluence of 4×10^{17} ions/m^2 leads to better results than a lower fluence of 8×10^{16} ions/m^2, although the island density observed at half monolayer coverage is the same. It seems that in the heteroepitaxial case, the enhancement in the island density is not the only parameter that determines the film quality.

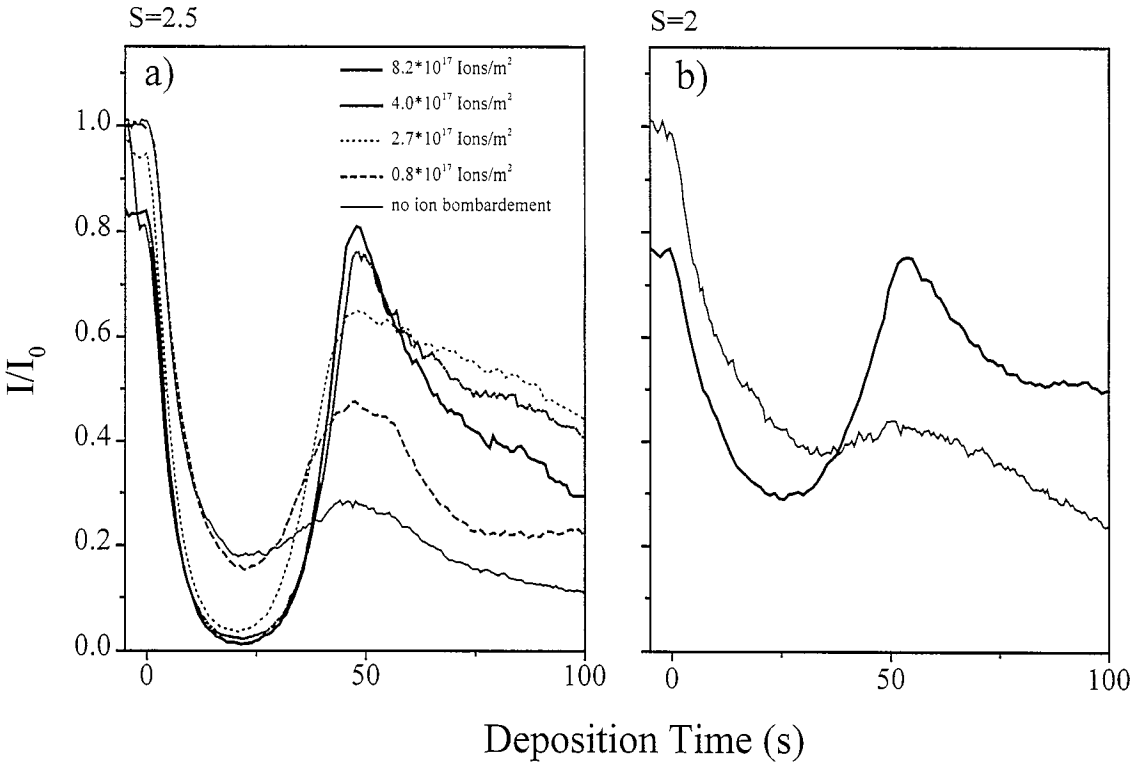

Fig. 11. Normalized anti-phase (a) and in-phase (b) He intensities during deposition of Ni at 300 K onto surfaces which were treated by ion bombardment with fluences as indicated. Deposition was carried out at a rate of $R=0.02$ ML/s.

Similar experiments at lower substrate temperatures also revealed strong oscillations and good layer-by-layer growth after soft sputtering [35].

To gain information about the density of defects during manipulated growth, in-phase growth curves were also taken, as shown in Fig. 11b. Growth on surfaces pre-sputtered with a fluence of 4×10^{17} ions/m^2 show a lower reflectivity in the first stage of growth. This is expected and is due to the higher step density on such surface due to the enhanced island density. However, at 1 monolayer coverage and beyond, the intensity reflected from manipulated films is significantly higher than that of the unmanipulated. Obviously, at higher coverages the defects created by sputtering are insignificant in comparison with the step density evolving during the imperfect natural growth. Not only is the layer distribution better for the manipulated films, but the defect density is also lower. However, the better *surface* of the films might be traded for a slightly roughened film–substrate *interface*. The nuclei created by sputtering consist of Cu and not Ni atoms and some vacancies in the substrate Cu layer are also created. Thus, growth on pre-sputtered surfaces might cause a rougher interface between the substrate and the film. This roughness, however, is rather small since the dose used corresponds to sputtering of only 0.08 ML [9]. To grow equally smooth films in unmanipulated growth, temperatures well above 375 K are needed [12] at which strong intermixing and even an upsweep of a complete Cu cap-layer may occur [17]. Presumably, these diffusion processes will lead to an even rougher interface between film and substrate.

Besides the fact that pre-sputtering leads to smoother film surfaces, one can learn from the enhanced amplitude of the growth oscillation that the Cu nuclei in the first layer do not give rise to preferential nucleation in the second layer. The Ni

adatoms landing on top of the growing Ni islands with a Cu nucleus in the centre are not trapped at the contact line between the Cu and Ni, but are efficiently diffusing over the step edge to fill the first layer.

Growth manipulation by ion bombardment was also used to grow several layers in layer-by-layer fashion. Before deposition and during deposition at maxima of the reflected anti-phase He intensity, i.e. at layer completion, ion pulses of 4×10^{17} ions/m^2 were given. As can be seen in Fig. 12, this leads to clear oscillations. In this way, the island density is enhanced in each new layer and the film grows two dimensionally. Compared to the unmanipulated growth at that temperature, the film has a better filling of the lower layers, as can be concluded from the higher anti-phase intensity upon monolayer completion. The unmanipulated film grows in a multilayer mode which leads to many open layers even in thin films. Similar results are obtained for all growth temperatures tested, i.e. between 250 and 350 K.

Anti-phase SPALEED profiles of the (00)-spots taken from films grown with the aid of sputter pulses showed no six-fold star-like pattern, but a round and sharp peak as expected from a flat film. With an FWHM of the (00) spot of only 1.4% SBZ, manipulated films of the thickness of 2 ML were of much higher quality compared with those naturally grown, which display an FWHM of 2.5%

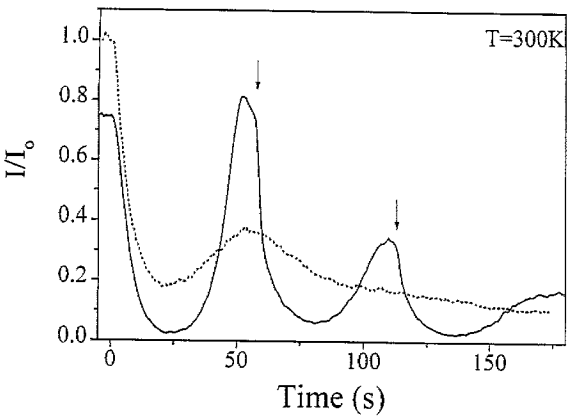

Fig. 12. Normalized anti-phase He intensity during deposition of Ni at 300 K. Sputter pulses of 4×10^{17} ions/m^2 were given before deposition and at times indicated by arrows in the graph.

SBZ. A similar film flatness could be achieved by unmanipulated growth only when the temperature is chosen well above the intermixing temperature, e.g. natural growth of a 2 ML Ni film at 440 K results in a FWHM of the (00) spot of 1.3% SBZ. However, one should not forget that these films are covered with a Cu cup-layer and that due to the upsweep of Cu the interface between Ni and Cu is most likely to be neither sharp nor flat.

Besides natural and manipulated growth of Ni on Cu(111), we also tried to change the growth mode by using oxygen as a surfactant. In the best results, two-dimensional growth was obtained for the first layer. After that, the surface of the film roughens very quickly to become even rougher than unmanipulated growth. In no cases were the films as smooth as those obtained with growth manipulation (rate variation and pulsed ion beam assisted growth). The use of oxygen as a surfactant is by far inferior to the kinetic growth manipulation methods and only leads to reasonably good results for the first monolayer and hence is of no practical use.

As a conclusion, it can be said that Ni on Cu(111) grows three-dimensionally rough below the intermixing temperature and that growth manipulation by the concept of two mobilities does overcome this and leads to layer-by-layer growth below this temperature. The layer filling obtained by these methods is much better than that by conventional growth, resulting in flatter surfaces. In addition, the defect density on the surface is lower. A comparison between pulsed ion beam assisted deposition at intermediate temperatures and unmanipulated growth at elevated temperatures is in clear favour of the first, although some interface roughening may be caused by the sputtering. Furthermore, it has been demonstrated that the use of a second evaporator, which performs nucleation in a pulse of very high deposition rate, also promotes layer-by-layer growth. In principle, an even higher rate during nucleation should lead to similarly good results as pulsed ion beam assisted deposition, but without the side effects of interface roughening and intermixing, making this recipe the method of choice in heteroepitaxial growth manipulation.

References

[1] K. Meinel, M. Klaua, H. Bethge, J. Cryst. Growth 89 (1988) 477.
[2] P.C. Dastoor, J. Ellis, A. Reichmuth, H. Bullman, B. Holst, W. Allison, Surf. Rev. Lett. 1 (1994) 509.
[3] E. Bauer, Appl. Surf. Sci. 1112 (1982) 479.
[4] G. Ehrlich, F.G. Hudda, J. Chem. Phys. 44 (1966) 1039.
[5] R.L. Schwoebel, E.J. Shipsey, J. Appl. Phys. 37 (1966) 3682.
[6] G. Rosenfeld, B. Poelsema, G. Comsa, J. Cryst. Growth 151 (1995) 230.
[7] G. Rosenfeld, R. Servaty, C. Teichert, B. Poelsema, G. Comsa, Phys. Rev. Lett. 71 (1993) 895.
[8] G. Rosenfeld, N.N. Lipkin, W. Wulfhekel, J. Kliewer, K. Morgenstern, B. Poelsema, G. Comsa, Appl. Phys. A 61 (1995) 455.
[9] W. Wulfhekel, N. Lipkin, J. Kliewer, G. Rosenfeld, L. Jorritsma, B. Poelsema, G. Comsa, Surf. Sci. 348 (1996) 227.
[10] S. Esch, M. Breeman, M. Morgenstern, T. Michely, G. Comsa, Surf. Sci. 365 (1996) 187.
[11] S. Esch, M. Bott, T. Michely, G. Comsa, Appl. Phys. Lett. 67 (1995) 3209.
[12] U. Gradmann, Ann. Physik 13 (1964) 213.
[13] D.W. Gidley, Phys. Rev. Lett. 62 (1989) 811.
[14] J. Zhang, Z.L. Han, S. Varma, Surf. Sci. 298 (1993) 351.
[15] S.P. Tear, K. Röll, J. Phys. C 15 (1982) 5521.
[16] F. Huang, M.T. Kief, G.J. Mankey, R.F. Willis, Phys. Rev. B 49 (1994) 3962.
[17] S. Yang, M. Yu, G. Meigs, X.H. Feng, E. Garfunkel, Surf. Sci. 205 (1988) L777.
[18] B. Poelsema, G. Comsa, in: Scattering of Thermal Energy Atoms, Springer Tracts in Modern Physics, Springer, Berlin, 1989, p. 115.
[19] B. Poelsema, G. Mechtersheimer, G. Comsa, Surf. Sci. 111 (1981) 519.
[20] M. Henzler, Appl. Surf. Sci. 1112 (1982) 450.
[21] J. Wollschläger, J. Falta, M. Henzler, Appl. Phys. A 50 (1990) 57.
[22] J.A. Venables, Phil. Mag. 27 (1973) 697.
[23] J.A. Venables, G.D.T. Spiller, M. Hanbücken, Rep. Prog. Phys. 47 (1984) 399.
[24] K. Morgenstern, F. Besenbacher, J. Nørskov, Private communication.
[25] P. Stoltze, J. Phys. Condens. Matter 6 (1995) 9495.
[26] M. Bott, M. Hohage, M. Morgenstern, T. Michely, G. Comsa, Phys. Rev. Lett. 76 (1996) 1304.
[27] Y.F. Liew, Y.L. He, A. Chan, G.C. Wang, Surf. Sci. Lett. 273 (1992) L461.
[28] K. Lenarčič-Poljanec, M. Hodošček, D. Lovrić, B. Gumhalter, Surf. Sci. 251/252 (1991) 706.
[29] T. Michely, M. Hohage, M. Bott, G. Comsa, Phys. Rev. Lett. 70 (1993) 3943.
[30] M. Henzler, Private communication.
[31] K. Morgenstern, G. Rosenfeld, G. Comsa, Phys. Rev. Lett. 76 (1996) 2113.
[32] T. Michely, G. Comsa, Phys. Rev. B 44 (1991) 8411.
[33] M. Breeman, D.O. Boerma, Surf. Sci. 278 (1992) L110.
[34] T. Michely, C. Teichert, Phys. Rev. B 50 (1994) 11156.
[35] W. Wulfhekel, I. Beckmann, N. Lipkin, G. Rosenfeld, B. Poelsema, G. Comsa, Appl. Phys. Lett 69 (1996) 3492.